Article:

Wang, L. orcid.org/0000-0002-4627-6462, Jiang, L. orcid.org/0000-0002-1009-996X, Zhai, Z. orcid.org/0000-0002-4524-4215 et al. (3 more authors) (2025) Are deprived communities exposed to higher PM2.5 concentrations? Evidence from Cangzhou, China. Transportation Research Part D: Transport and Environment, 143. 104762. ISSN 1361-9209

https://doi.org/10.1016/j.trd.2025.104762

Are deprived communities exposed to higher $PM_{2.5}$ concentrations? Evidence from Cangzhou, China

Lewen Wang[a], Like Jiang[b], Zhiqiang Zhai[a], Lei Yu[a, c, d], Guohua Song[a, e], Yizheng Wu[a*]

[a] Key Laboratory of Transport Industry of Big Data Application Technologies for Comprehensive Transport, Beijing Jiaotong University, 3 Shangyuancun, Haidian District, Beijing 100044, P. R. China.

[b] Institute for Transport Studies, University of Leeds, UK.

[c] College of Science and Technology, Texas Southern University, 3100 Cleburne Avenue, Houston, Texas 77004, United States.

[d] Shandong Jiaotong University, Ji'nan 250357, P.R. China.

[e] MOE Engineering Research Center of Clean and Low-carbon Technology for Intelligent Transportation, Beijing Jiaotong University, 3 Shangyuancun, Haidian District, Beijing 100044, P.R. China.

*Corresponding author at:

Yizheng Wu: Beijing Jiaotong University, 3 Shangyuancun, Haidian District, Beijing 100044, P.R. China. Email address: wuyizheng@bjtu.edu.cn.

Abstract

Deprived communities tend to face higher environmental exposure risks due to inadequate environmental protection and economic investment. Estimating high-resolution disparities in pollution exposure is key to addressing such Environmental Justice issues. This study conducted a $PM_{2.5}$ measurement campaign in Cangzhou, China, in 2021, by using a taxi-based mobile sensing system. Disparities in pollution exposure, health impacts and related economic costs were calculated between deprived and affluent zones. The results showed mean values cannot represent the full extent of exposure inequality, and distributional characteristics should be emphasized. Pollutant concentrations and relative risks in some disadvantaged areas exceeded the maximum values in affluent areas. Disparities are more pronounced within deprived areas, with Gini coefficients for pollution exposure of 9.12%, exceeding affluent areas (2.28%). But affluent areas exhibit higher economic costs. The study contributes to portraying the inequalities of environmental exposure in developing country cities, helping formulate policies to mitigate environmental health disparities.

Keywords: Environmental justice, Health impact assessment, Deprived-affluent areas disparities, Roadside fine particulate matters, Mobile monitoring system

1. Introduction

Atmospheric fine particulate matters ($PM_{2.5}$) pose serious health risks. Exposure to high levels of $PM_{2.5}$ can lead to fatal health problems (WHO, 2016), such as cardiorespiratory diseases (Manisalidis et al., 2020), respiratory diseases (Orellano et al., 2020), pulmonary illnesses (Chen et al., 2017). The U.S. Environmental Protection Agency states a link exists between $PM_{2.5}$ and mortality rates (US EPA, 2019). Given these health damages, the WHO has adjusted the long-term exposure level for $PM_{2.5}$ in the Global Air Quality Guidelines from 10 μg/m^3 to 5 μg/m^3 in 2021. However, about 90% of the global population still live in areas with $PM_{2.5}$ exceeding 10 μg/m^3 in 2019 (WHO, 2021).

The truth is that pollutants are not evenly distributed between regions. Socio-economically deprived areas exhibit elevated pollutant levels, and deprived groups face higher risks of environmental exposure (Lim et al., 2012; Badland and Pearce, 2019). The unequal socio-spatial dispersion of air pollution highlights Environmental Justice (EJ) concerns (Hsu et al., 2021; Fang et al., 2023). EJ means that no individual shoulders a disproportionate burden of adverse environmental effects due to policy or economic disadvantages. EJ associated with air pollution is frequently investigated in developed urban cities. Exposure to traffic-related pollution was shown to be highest among the most disadvantaged groups in New Zealand (Kingham et al., 2007). A non-linear relationship between higher pollutant concentrations and deprived areas was found in Los Angeles (Molitor et al., 2011). A significant positive correlation between $PM_{2.5}$ concentrations and Social Deprivation Index existed in Hong Kong (Li et al., 2018). However, the above studies lack the context of small and medium-sized cities, whose populations may be growing faster than large urban clusters (Berdegué and Soloaga, 2018), but inequalities in pollution exposure in such cities remain unclear. Furthermore, the majority of comparisons focus on affluent and deprived areas, neglecting the disparities within these regions.

High-resolution $PM_{2.5}$ data are essential for EJ implementation. However, limited by measurement methods, most studies used fixed monitoring stations data or air pollution estimation models to evaluate pollution exposure. The global average population distance to the nearest $PM_{2.5}$ fixed monitoring station is 220 km (Martin et al., 2019). Fixed monitoring stations are usually situated in bustling urban centers (Stampfer et al., 2020). Due to this sparse spatial distribution, large-scale air pollution monitoring is difficult to achieve, especially in economically disadvantaged areas (Hao et al., 2022). However, pollutants at the neighborhood scale are spatio-temporally dynamic and can change dramatically over short distances with short periods (Hoek et al., 2008; Apte et al., 2017). Such variability cannot be captured by fixed monitoring stations. Given that individuals predominantly reside and work in these street-level environments, using high-resolution pollutant data to accurately estimate their health impacts and disparities is a necessary but challenging task (Wu et al., 2023). The utilization of low-cost sensors in conjunction with mobility has emerged as a prevalent approach for monitoring air pollution, such as being carried by trained individuals or mounted on motorcycles and probe vehicles (Targino et al., 2016; Qiu et al., 2017; Munir et al., 2022; deSouza et al., 2023). In addition, mobile monitoring with sensors installed on the overhead lights of taxis enables high-resolution data collection with good accuracy. It provides a basis for expanding the sampling space and conducting fine-grained health impact assessments and disparities (Wu et al., 2020; Yu et al., 2022; Wang et al., 2024).

Moreover, inequalities in pollution exposure will exacerbate inequalities in income, physical health, and well-being, significantly compromising equity in safeguarding individuals' health and welfare. Such health inequalities can even reduce employment and productivity and create severe psychological stress in deprived areas, further exacerbating impoverishment (Marmot, 2020; Tao et al., 2021). However, existing environmental policies mainly focus on the sources of pollutants and their concentrations, ignoring the disproportionate adverse environmental impacts on populations and failing to adopt a health-oriented perspective. Most people do not have a quantified concept of the human health costs of air pollution and some studies have attempted to estimate the related public welfare costs to provide a basis for the development of environmental health compensation mechanisms and supporting legislation (Maji et al., 2018; Yang et al., 2019; Zhang et al., 2020, 2008). However, the existing studies about economic costs have been conducted mainly on a macro scale and lack assessment among different socio-economic groups. While EJ emphasizes the inequality of environmental burdens, the EJ further implies that remedies are needed to mitigate the injustices imposed on disadvantaged groups. The United Nations Sustainable Development Goals (United Nations, 2019) have outlined a vision to diminish inequalities. Goal 3 on Good Health and Well-being emphasizes the need to protect vulnerable groups living in areas with a high disease prevalence. Goal 10, Reduced Inequalities, states the necessity of working to reduce inequalities. However, deprived areas are more likely to be trapped in a situation where they live in highly polluted environments, where their health is affected, their welfare is jeopardized, their employment opportunities are reduced, and they become poorer. Such inequality may even strengthen fertility among vulnerable groups, exposing more people to such hazards (Islam and McGillivray, 2020). 575 million people are predicted to live in extreme poverty worldwide by 2030 (United Nations, 2019). Therefore, conducting assessments of disparities in pollution exposure, health impacts and economic costs will help to develop targeted and equitable air pollution prevention strategies that reduce disparities between regions and socio-economic groups.

Although studies have been conducted to examine inequalities in pollution exposure among different socio-economic groups, most of them have been carried out in larger and more developed cities and have used low-resolution pollution concentration data. Gaps exist in research on small and medium-sized cities where the distribution patterns of population and pollution could be very different from those in larger and more developed cities. The fine-grained inequalities in pollution exposure, health effects and economic costs, along with disparities within areas of different socio-economic positions, remain unclear. Therefore, this study aims to contribute to this knowledge gap, and the major contributions of our work are highlighted below:

1. Hyper-localized $PM_{2.5}$ concentrations across extensive spatial extents and long durations were collected by a taxi-based mobile atmospheric monitoring system in both low and high socio-economic position communities in a medium-sized city in China.

2. More accurate and fine-grained $PM_{2.5}$ was used for EJ study. Disparities in pollutant concentrations, health risks, and $PM_{2.5}$-related deaths between deprived and affluent areas were estimated. Inequalities in exposure within regions were discussed. High-resolution maps of roadside $PM_{2.5}$ concentrations and relative risks were created, and refined health impacts were implemented. Distribution pictures of inequalities in environmental exposures and health effects were developed.

3. The fine-grained $PM_{2.5}$-related economic costs were calculated for regions with different socio-economic status. Potential causes and hazards of disparities in pollution exposure, health effects, and economic costs were discussed, and measures for improvement were proposed.

2. Materials and methods

Our research includes five steps: (1) define the study region, (2) collect data, including high-resolution $PM_{2.5}$ concentration data, population and housing price data, (3) estimate fine-grained health effects, (4) quantify the economic costs of those impacts, (5) assess the disparity, including pollutant concentration and pollution exposure between areas. The following describes these steps in detail.

2.1. Study area

This study was conducted in Cangzhou, a city located in Hebei Province, China. Cangzhou was chosen as it is a heavily industrialized city in the Beijing-Tianjin-Hebei region and an area facing serious air pollution issues. It is a typical medium-sized city with a population of 810,000, according to Tabulation on 2020 China Population Census by County, characterized by central area being economically developed and densely populated compared to suburbs. As shown in **Figure 1 (a),** Xinhua District, Yunhe District and Cang County are three of the districts and counties in Cangzhou.

2.2. Data collection

2.2.1. Source of population data

The study area was divided into 2,763 1km×1km grid cells, as shown in **Figure 1 (c)** and **(d)**. The population data were sourced from WorldPop (https://www.worldpop.org/datacatalog/), an organization affiliated with the University of Southampton in the UK, dedicated to providing an open platform for high-resolution global population distribution data. The raw data are provided in TIFF format as raster files, with each pixel value representing the population count within its corresponding area. After downloading, the data were integrated into GIS, refined to the study area through mask extraction, and converted into SHP format by raster-to-vector transformation to obtain population data. More details can be seen in **Supplementary Materials.**

2.2.2. Source of housing price data

Existing studies have used census-level income data to classify populations into different socioeconomic status groups (Rowangould, 2013; Antonczak et al., 2023). However, such data in China is not publicly available. Research has shown that income impacts housing affordability, as housing constitutes a substantial portion of household expenditures (Määttänen and Terviö, 2014; Mirkatouli et al., 2018). Housing loans represent 75.9% of total household liabilities in China, according to a survey conducted by Statistics and Analysis Department of the People's Bank of

China. The relationship between housing prices and income also influences household consumption levels, savings, and other factors (Berger et al., 2018;Atalay and Edwards, 2022).

A positive correlation has been identified between residents' socioeconomic status and housing prices (Mirkatouli et al., 2018). Using housing price levels to classify populations into high and low socioeconomic status groups is a common approach when income data is unavailable (Coffee et al., 2013). In the study by Guo et al. (2020b) and Ding et al. (2023), this method was used to analysis the equity of pollution exposure and health impacts. Therefore, given the difficulty in obtaining census level income data, our study adopts housing price levels to classify populations into high and low socioeconomic status groups.

The housing price data were sourced from Anjuke, a leading real estate information service platform in China (www.anjuke.com). The platform comprehensively covers listings for new homes, second-hand properties, and rental units. We collected housing prices and geographical locations from 887 residential areas and made them into a dataset. The housing prices range from 540 to 30,071 yuan/m^2. House prices are not shown in some areas as some are self-built houses. Residing in self-built houses is common in China (especially in small or medium-sized cities like Cangzhou) due to their affordability and the absence of security and property management fees typical in residential communities (see **Figure S4** for more details). Therefore, we classified regions with housing prices exceeding the average as high socio-economic position communities, and regions with prices below the average and lacking housing prices as deprived areas, as shown in **Figure 1 (d)**.

2.2.3. Source of roadside $PM_{2.5}$

Roadside $PM_{2.5}$ data were collected using a taxi-based mobile atmospheric monitoring system. The detector is an SDS019-TRF laser particle sensor developed based on laser diffraction theory by Shandong Nova Fitness Co., Ltd. The silicone tube resin material was upgraded, shock-absorbing screws were installed, and pre-deployment testing was conducted to mitigate the impacts of high-temperature environments, vibrations, and strong winds. Four sensors were mounted on the headlight of the taxi, and the reliability of the monitoring dataset was ensured through automatic fault detection by cross-checking. The device utilizes a dual-mode GPS and Beidou positioning system with an accuracy of less than 20 meters, and each monitoring device can upload $PM_{2.5}$ data every 3 seconds, returning latitude, longitude, timestamp, and $PM_{2.5}$ concentration values. In our previous research (Wu et al., 2020), the validity of the data was confirmed through spatiotemporal comparisons with fixed monitoring stations using five statistical metrics, including relative error (E_r), fractional bias (FB), normalized mean square error, geometric variance (VG), correlation coefficient (R), and the fraction of predictions within a factor of two of the observations (FAC2). In 2021, the system was deployed on 54 taxis, collecting a total of 79,973,505 valid data, with more than 10 million data for each season. Data monitoring was conducted continuously over 24 hours, with minimum hourly data exceeding 30,000 in each season. All major roads were covered, and good spatial and temporal coverage was achieved in the study area. More details can be found in the **Supplementary Materials**.

Each 1km×1km grid cell was statistically analyzed to demonstrate the availability of monitoring data. **Equation (1)** was used to calculate the proportion of the population covered by monitoring, and **Equation (2)** was applied to assess the variation coefficient within each grid.

$$r = (\sum pop_{cell}/POP) \times 100 \tag{1}$$

Where r is the proportion of population covered by monitoring, ranging from 0 to 100, with larger values indicating more people covered. POP is the total population of study area. pop_{cell} is the grid population with monitoring data.

$$CV_{cell} = \sigma_{cell}/\mu_{cell} \tag{2}$$

Where CV_{cell} is the variation coefficient of each cell, $CV_{cell} < 1.5$ indicates that the variability between data points is not very high and the data is relatively stable; σ_{cell}, μ_{cell} are the standard deviation and mean of all roadside $PM_{2.5}$ sampling data for each cell, respectively.

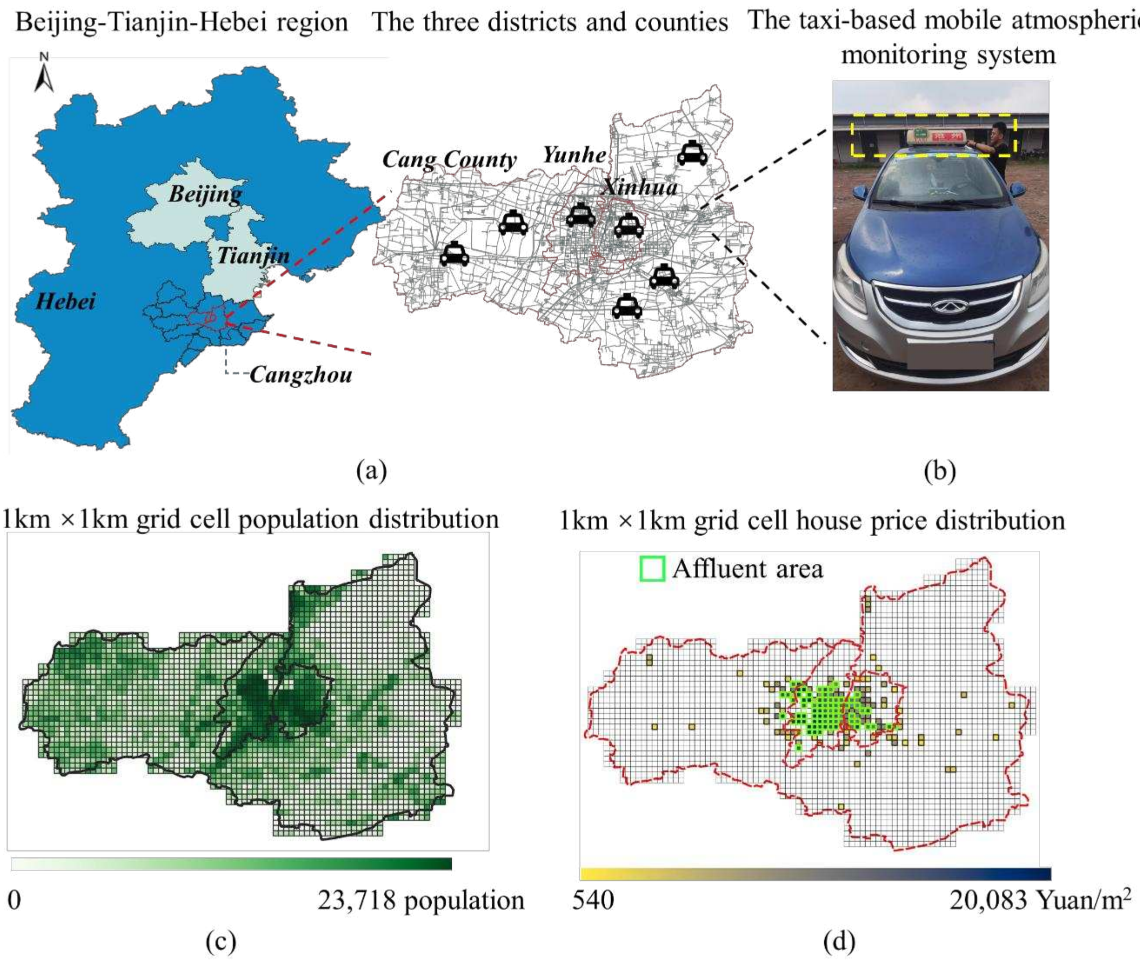

Figure 1 Study area. (a) The location of the study area. (b) The taxi-based mobile atmospheric monitoring system. (c) 1km×1km grid cells population. (d) 1km×1km grid cells housing price distribution.

2.3. Health impact assessment

In this study, the epidemiologic relative risk (RR) was applied to estimate the long-term health effects attributable to roadside $PM_{2.5}$ exposure. This method is recommended by the Global Burden of Disease (GBD) (Pisoni et al., 2023) and is calculated as follows.

$$HI_{cell,i} = AF_{cell,i} \times Pop_{cell} \times B_i \tag{3}$$

$$AF_{cell,i} = (RR_{cell,i} - 1)/RR_{cell,i} \tag{4}$$

Where $HI_{cell,i}$ is the health impacts of health outcomes i in each cell; $AF_{cell,i}$ is defined as the population attributable fractions for health outcomes i in each cell; Pop_{cell} is the gridded population data; B_i is the baseline disease-specific health impacts rate for health outcomes i, and obtained from the China Health Statistical Yearbook; $RR_{cell,i}$ is the relative risks (RRs) of health outcomes i in each cell, and if $RR_{cell,i} > 1$ indicates adverse health effects. This research considered long-term exposures and calculated mortality for four health outcomes, including all-cause, cardiovascular, respiratory and lung cancer mortality.

Three RR estimation functions have been developed for $PM_{2.5}$ exposure, including the integrated exposure risk (IER) (Burnett et al., 2014), log-linear (LL) exposure-response functions (Pascal et al., 2013) and the non-linear power law (NLP) function (Chowdhury and Dey, 2016). The LL function is the recommended model for estimating health effects in high PM pollution areas (WHO, 2006) and is currently the most widely used exposure response model in China (Lin et al., 2017; Yin et al., 2017; Maji et al., 2018; Wang et al., 2024), calculated as **Equation (5)**.

$$RR_{cell,i} = \exp\,[\beta_i \times (\bar{c}_{cell} - c_0)] \tag{5}$$

Where β_i is the exposure response coefficient, meaning the incidence change of health outcomes i per μg/m^3 $PM_{2.5}$ increment, obtained from the Chinese epidemiological study (shown in **Table 1**); $\bar{c}_{cell}$ is the average $PM_{2.5}$ concentration in each cell; c_0 is the baseline $PM_{2.5}$ concentration, and is set to be 5 μg/m^3 according to the latest version of the WTO Air Quality Guidelines (WHO, 2021).

To calculate the annual mean $PM_{2.5}$ concentrations, grid cells with monitoring data for all seasons were selected. The average $PM_{2.5}$ concentration in each cell is calculated as **Equation (6)**.

$$\bar{c}_{cell} = \sum_{n=1}^{N_{cell}} p_{cell,n} / N_{cell} \tag{6}$$

Where $p_{cell,n}$ is the $PM_{2.5}$ concentration for the nth monitoring point in each cell; N_{cell} is the total number of monitoring data in each cell.

Table 1 β for four health outcomes for long-term exposure.

Health outcomes	β_i (CI 95%) (Fang et al., 2016)
All-cause mortality	5.37 (3.48,7.27)
Cardiovascular mortality	5.91 (3.63,8.18)
Respiratory mortality	2.54 (0.95,4.12)
Lung cancer mortality	8.93 (4.32,13.55)

2.4. Economic valuation of $PM_{2.5}$ health impacts

The value of statistical life (VSL) is a widely available indicator used to monetize the ultimate impact on health due to air pollution. It is defined as the aggregating individuals' willingness to pay (WTP) to secure a marginal reduction in the risk of premature death, which is not the value of a person's life, but the sum of an individual's WTP (OECD, 2014). The VSL can be calculated as **Equation (7)**.

$$VSL = \partial WTP / \partial R \tag{7}$$

Where ∂WTP represents individuals' willingness to pay; ∂R represents a small eduction of mortality risk.

Existing studies in China have focused mainly on Beijing or nationwide, lacking localized WTP (Zeng et al., 2024). The calculation methodology recommended by the OECD incorporates parameters such as income elasticity, GDP per capita, and consumer price index (CPI), shown in **Equation (8)**. Economic costs associated with health endpoints in different regions and years can be estimated by using a baseline (base region and base year). This method has been widely applied to estimate health-related economic costs due to air pollution (OECD, 2014; Giannadaki et al., 2018; Wang et al., 2020; Zeng et al., 2024). Therefore, this study calculated the economic cost of the four health endpoints in each grid cell in Cangzhou based on the existing health-related cost data in Beijing (Guo et al., 2010; Yin et al., 2017; Maji et al., 2018; Zeng et al., 2024).

$$VSL_{cell} = VSL_{(t)} \times (G_{cell,(t)}/G_{(t)})^{\tau} \times (1 + \%\Delta P + \%\Delta G_{cell})^{\tau} \quad (8)$$

Where VSL_{cell} is the per unit economic cost in each cell in Cangzhou in 2021; $VSL_{(t)}$ is the per unit economic cost in year t in the baseline area (e.g., Beijing is usually chosen); $G_{(t)}$ is the per capita GDP of Beijing in year t; $\%\Delta P$ is percentage alteration in CPI from year t to 2021, data source from Hebei Statistical Yearbook (more details shown in **Table S1** of Supplementary Material); $G_{cell,(t)}$ is the per capita GDP for each cell in year t; $\%\Delta G_{cell}$ is percentage alteration in GDP per capita from year t to 2021 in each cell. We used grid cell population data and GDP data to calculate. The gridded GDP data were obtained from the Resource and Environmental Science Data Platform ((http://www.resdc.cn/DOI),2017.DOI:10.12078/2017121101). The distributions of gridded GDP and more details can be seen in **Figure S8**. τ is the income elasticity, which is set at 0.8 according to OECD (2014).

Thus, the economic costs can be calculated as **Equation (9).**

$$EC_{cell,i} = VSL_{cell,i} \times HI_{cell,i} \quad (9)$$

Where $EC_{cell,i}$ is the economic costs for health outcomes i in each cell; $HI_{cell,i}$ is the health impacts of health outcomes i in each cell.

2.5. Estimation of disparity

2.5.1. The disparity in $PM_{2.5}$ concentration between regions

Equation (10) was used to calculate the disparities in concentration between two areas.

$$\begin{gathered}\lambda_{diff} = N_{(s)}/N_{a,cell} \times 100\% \\ s = \{c_{a,1}, \dots, c_{a,i}, \dots\}, c_{a,i} > c_{b,max}\end{gathered} \tag{10}$$

Where λ_{diff} is defined as the disparities in concentration between areas a and b; $N_{a,cell}$ is the total number of grid cells in area a; $N_{(s)}$ is the number of set s; $c_{b,max}$ is the maximum concentration of grid cells in area b; s is the set of area a with grid cells concentration above $c_{b,max}$; $c_{a,i}$ is the concentration in area a. In our study, area a and area b refer to deprived area and affluent area, respectively.

2.5.2. The Gini coefficient in pollution exposure

The Gini coefficient is frequently employed to quantify economic inequality (Atkinson, 1970). The same concept can be used to assess disparities in pollution exposure (Pisoni et al., 2022).

$$G_s = 1/(2\mu_s) \times \sum_{i=1}^{C_s} \sum_{j=1}^{C_s} p_i p_j |\bar{c}_i - \bar{c}_j| \tag{11}$$

$$\mu_s = \sum_{i=1}^{C_s} p_i \bar{c}_i \tag{12}$$

Where G_s is the Gini coefficient in deprived or affluent areas, ranging from 0 to 1, with higher values representing increased inequality; s indicates deprived or affluent areas; C_s is the total number of grid cells; $\bar{c}_i$ and $\bar{c}_j$ are the average concentration of cell i and j; p_i and p_j are the proportion of population in cell i and j.

3. Results

3.1. Statistical information of sampling data in each grid cell

High coverage of monitoring was achieved within 1km × 1km grid cells. As shown in **Figure 2 (a)**, the number of grid cells with monitoring data each month exceeds 1,000. The proportion of the population covered by monitoring (r) each month exceeds 70%. In **Figure 2 (b)**, the average number of monitoring data per grid cell in spring, summer, autumn, and winter is 12,225, 10,528, 9,862 and 8,148, respectively. **Figure 2 (c)** shows the coefficient of variation for each grid. In each season, the proportion of grids with $CV_{cell} > 1.5$ is less than 1% (shown in Figure 2 (**d**)), indicating that the monitoring data varies within a reasonable range under the restricted temporal and spatial scopes.

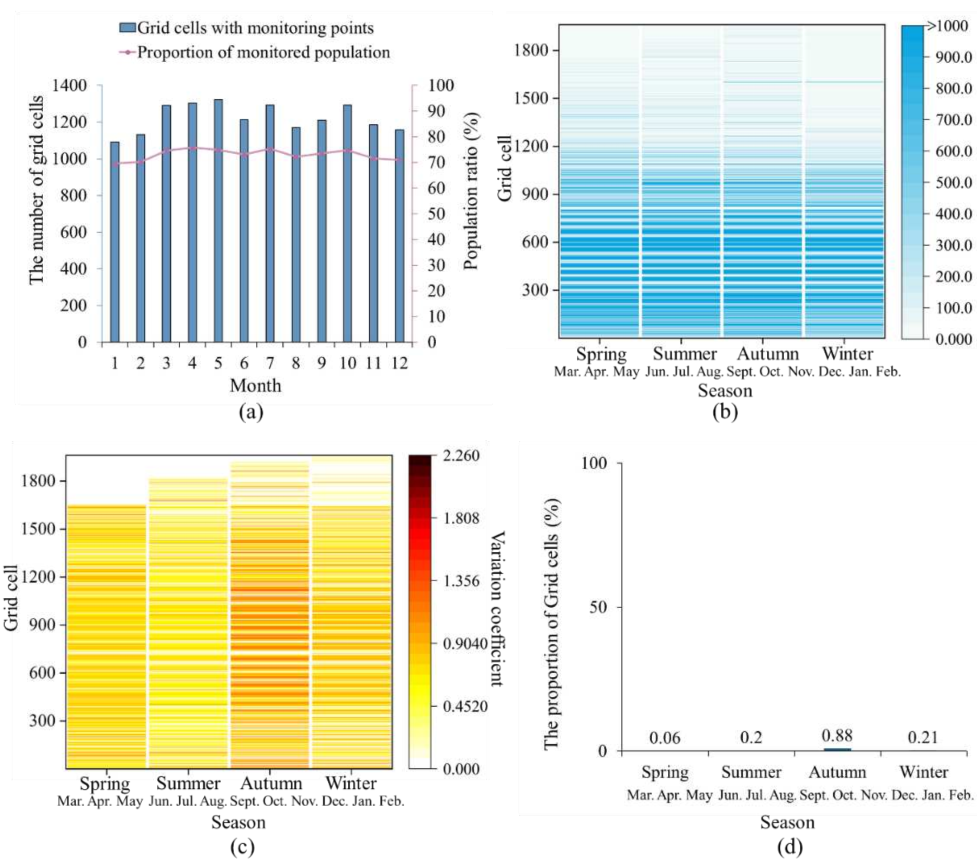

Figure 2 Statistical information of roadside $PM_{2.5}$. (a) Number of grid cells with monitoring

data per month and population coverage proportion. (b) The number of monitoring data in each cell. (c) The coefficient of variation in each cell. (d) The proportion of coefficient of variation exceeding 1.5.

3.2. The disparities in concentration

Due to objective limitations, not all grid cells under the 1km×1km resolution were monitored (e.g., mountainous or forested regions that were difficult to access). However, the monitored areas covered over 70% of the population. Grid cells with monitoring data available for all four seasons were selected, including 1,102 grid cells in low housing price areas (representing 55.1% of the total population) and full coverage of the 78 grid cells in high housing price areas (representing 16.56% of the population). **Figure 3 (a)** presents a refined pollution concentration map at 1 km×1 km resolution, illustrating the spatial and temporal variability of pollutant concentrations. Significant variations in roadside $PM_{2.5}$ concentrations can be observed between adjacent grid cells within the same season. Also, a single grid's concentration may exhibit substantial changes across different seasons. However, the limited spatial coverage of stationary monitoring stations fails to capture such dynamic, potentially exposing populations to elevated and variable pollution levels without their awareness.

As shown in **Figure 3 (b)**, the average concentrations in deprived areas are close to affluent areas. However, disparities in pollutant concentration distribution between the two regions are evident. Air pollution levels are more widely distributed in underdeveloped areas. The maximum $PM_{2.5}$ concentrations in deprived areas are much higher than affluent areas in all seasons. The highest concentrations in deprived communities were 155.60 μg/m^3, 113.55 μg/m^3, 150.68 μg/m^3, and 174.93 μg/m^3 in spring, summer, autumn, and winter, respectively, while in affluent areas were

50.62 μg/m^3, 39.68 μg/m^3, 52.02 μg/m^3, and 75.04 μg/m^3, respectively. Specifically, we calculated the percentage of cells within deprived regions where concentrations surpass the maximum values in affluent areas, according to **Equation (10)**. The λ_{diff} for four seasons were 17.97%, 5.72%, 15.25%, and 9.89%, respectively. Residents of these deprived regions (accounting for 5.99%, 2.29%, 5.25%, and 3.56% of the total population, respectively) live with pollution concentrations exceeding the highest concentrations in affluent areas, posing significant inequalities in air pollution exposure. The actual values would be higher than these proportions, as concentrations in some deprived areas were not monitored. However, average concentrations of pollutants fail to capture such exposure differences, and environmental protection efforts in economically disadvantaged areas can easily be overlooked. Addressing environmental justice in regions with different socioeconomic positions needs to map inequalities across full exposure distributions.

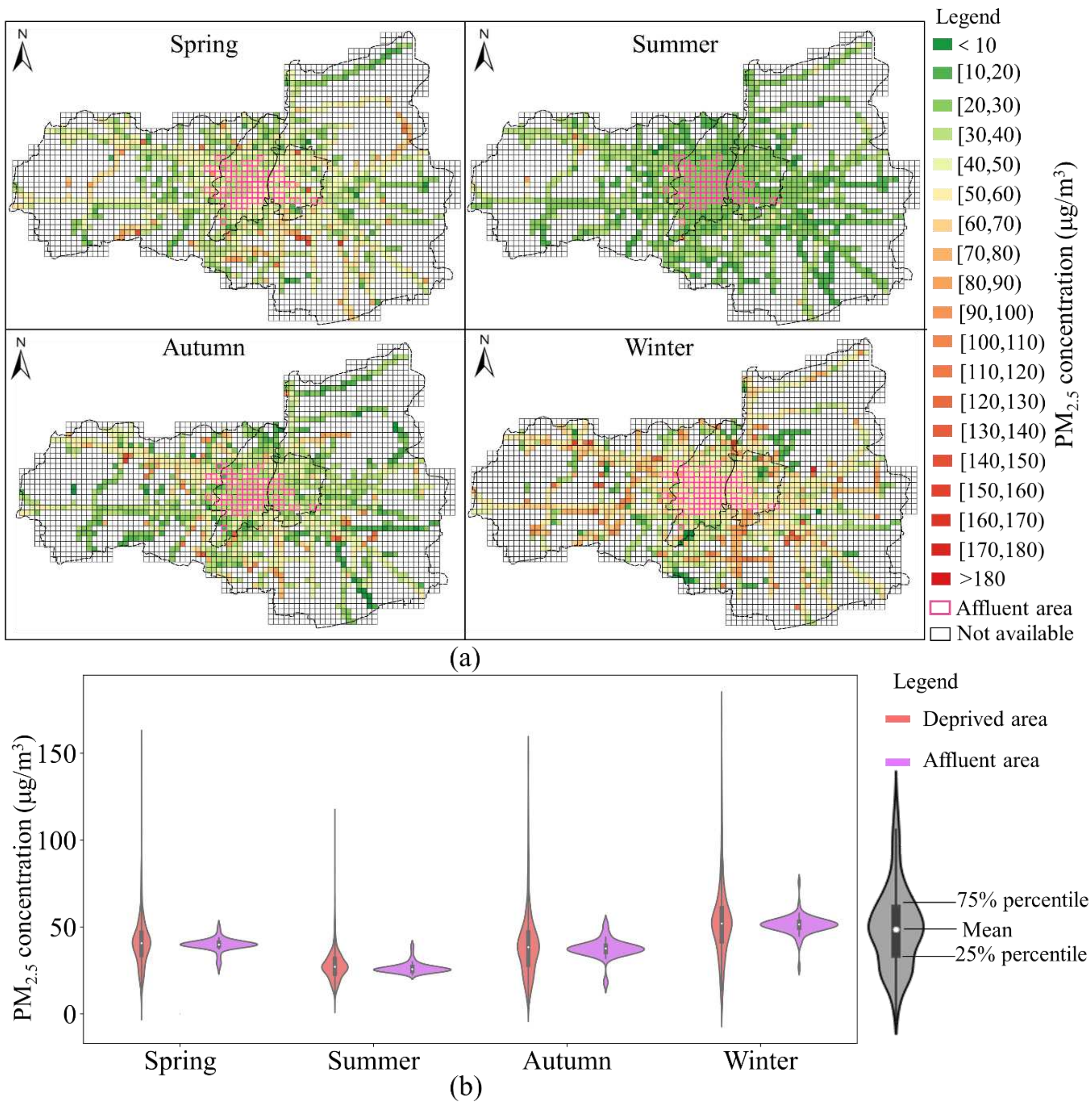

Figure 3 The disparities in concentration. (a) High-resolution roadside $PM_{2.5}$ concentration maps. (b) The disparities between deprived and affluent areas.

3.3. The disparities in health impact

According to **Equations (3)** to **(6)**, we calculated the health impacts in grid cells containing the four health outcomes of all-cause mortality, cardiovascular mortality, respiratory mortality, and lung cancer mortality. As shown in **Figure 4 (a)**, the RRs of all grids are more than 1, indicating negative health impacts. The refined health impact distribution maps show that RRs are lower in affluent areas. Some grids in deprived areas have RRs of (1.2, 1.3] for all-cause mortality, (1.3, 1.4] for cardiovascular mortality, (1.1, 1.2] for respiratory mortality, and risks of lung cancer mortality above 1.8, which exceeds the RRs for most grids in communities with high socio-economic positions.

Figure 4 (b) shows the disparities of RRs between the two areas. The average RRs in underdeveloped areas of all-cause, cardiovascular, respiratory and lung cancer mortality were 1.211, 1.235, 1.095, and 1.378, respectively, and 1.199, 1.221, 1.089, and 1.352 in affluent areas. 23.91% of grid cells in deprived areas have higher health risks for the four health outcomes than the highest values in communities with high socio-economic positions. Individuals living in communities with lower socio-economic positions suffer a higher risk of $PM_{2.5}$-related mortality.

Combined with the grid cells population dataset, the number of $PM_{2.5}$-related deaths was calculated. The percentage of deaths attributed to all-cause, cardiovascular, respiratory, and lung cancer in these three districts of Cangzhou was 0.142% (1,713 deaths), 0.033% (403 deaths), 0.005% (65 deaths), and 0.014% (180 deaths), respectively. This result is reasonable, and some health impact studies have been conducted in Hebei Province, reporting more than 30,000 $PM_{2.5}$-related deaths (including all-cause, cardiovascular diseases, respiratory diseases, and lung cancer) in some cities in 2013 (Fang et al., 2016) and 676,000 $PM_{2.5}$-related deaths caused by lung cancer in 2016 (Maji et al., 2018). Specifically, affluent areas had 378, 89, 14, and 40 deaths, accounting for 0.031%, 0.007%, 0.001%, and 0.003% of the total population, respectively. And deprived areas accounted for 0.111% (1,335 deaths), 0.026% (314 deaths), 0.004% (51 deaths), and 0.012% (140 deaths). However, the actual values for deprived areas would be even higher, as some grids were not monitored, whereas affluent areas achieved full coverage. More deaths occur in deprived communities, and health impacts vary unequally among social groups.

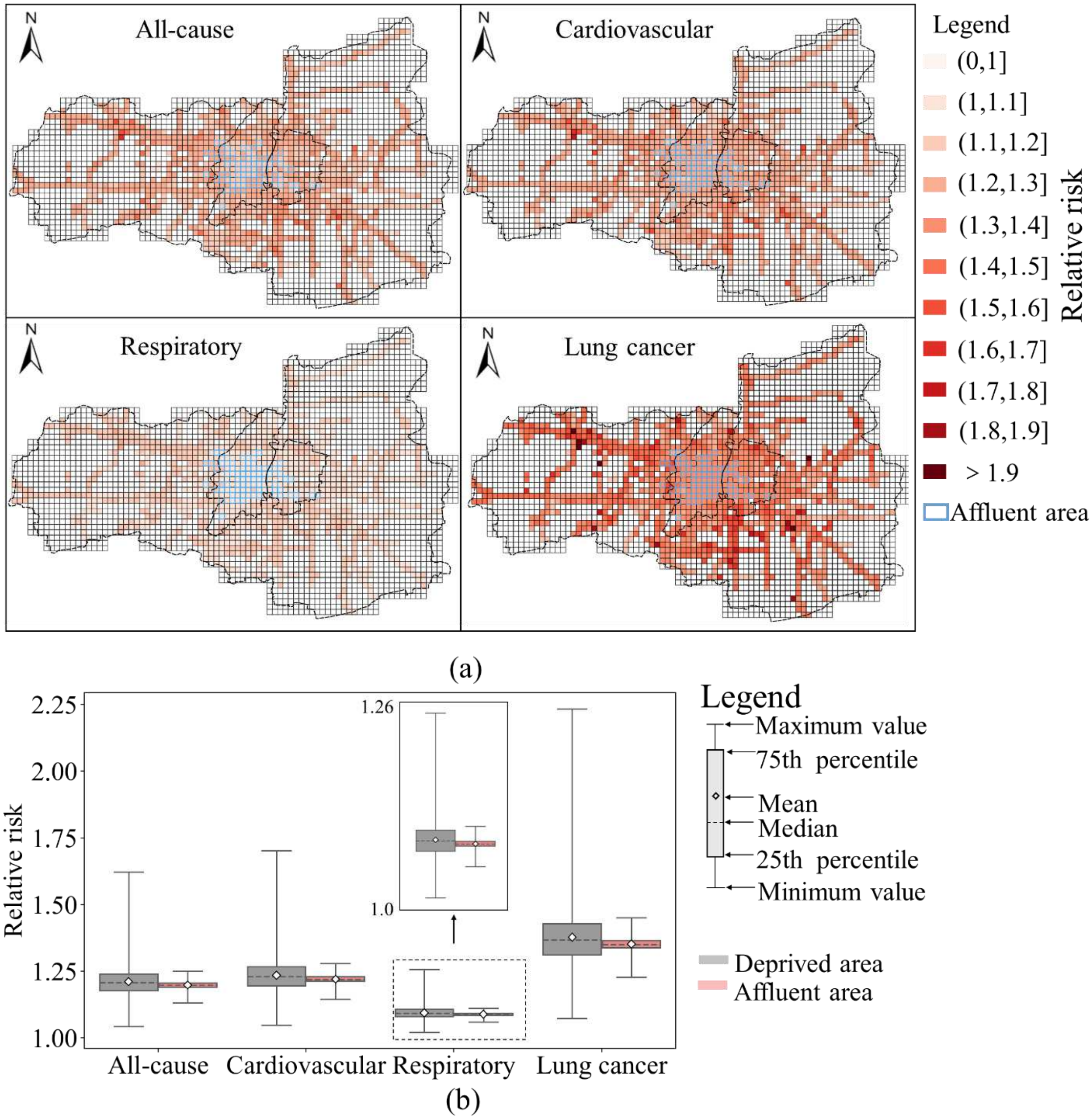

Figure 4 The relative risks of four health endpoints. (a) Fine-grained distribution of health impacts. (b) The difference between deprived and affluent areas.

3.4. Economic valuation of $PM_{2.5}$ health impacts

Figure 5 (a) shows the spatial distribution of VSL_{cell}. Overall, the VSL_{cell} is higher in affluent areas (1,216,652 USD) than in deprived areas (475,763 USD). People in communities with high socio-economic positions have a stronger willingness to pay. Some deprived regions also show a higher willingness to pay, as these grids have smaller populations (shown in **Figure 1 (c)**) and are clustered with multiple factories with higher GDP (see **Figure S8**), leading to higher GDP per capita and VSL_{cell}. The economic cost of different health endpoints varies, with all-cause mortality incurring the highest, followed by cardiovascular and lung cancer mortality, and respiratory mortality being the lowest, as shown in **Figure 5 (b)**. The economic costs are higher in affluent areas, with the four health outcomes being 2,396,331, 564,447, 91,145, 252,120 USD, respectively, while in deprived areas are 567,660, 133,624, 21,668, 59,479 USD.

The result reflects the fact that the rich are more willing to pay for mitigating health damage, and people with high socio-economic positions value self-protection investments more than low-income people; for example, one study showed that the rich are more likely to invest in air filters (Sun et al., 2017). This difference in individual preventive spending implies that inequalities in socio-economic status will continue to increase disparities in air pollution exposure. For example, the rich are more likely to own cars, shielding them from environmental pollution, while disadvantaged groups are more prone to commuting by motorcycle, increasing the risk of outdoor exposure. In addition, individuals with lower skill levels often engage in outdoor professions like street cleaning and package delivery. In contrast, high-skilled workers typically work indoors, reducing outdoor exposure time (Sun et al., 2017; Kim et al., 2024). Residents of underdeveloped areas are also inclined to work in agriculture, as data from Cangzhou Statistical Yearbook shows that the power of agricultural machinery in deprived areas far exceeds affluent areas. Individuals in deprived areas are more likely to be directly exposed to emissions from agricultural diesel equipment. Health inequalities between regions will continue to widen if no targeted measures are taken. Many people do not have this quantified concept of the human health costs caused due to air pollution and are unaware of such disparities. Goals for reducing pollution exposure in deprived regions are still lacking in many countries' policy frameworks and action programs.

Moreover, $PM_{2.5}$ has caused severe economic damage globally. The economic cost caused by $PM_{2.5}$ in China amounted to 101.39 billion USD in 2016 and 86.887 billion USD in 2017 (Maji et al., 2018; Sun et al., 2022). The cost of deaths caused by $PM_{2.5}$ in 26 European cities was €7.8 billion in 2019 (Belis et al., 2023). 26.805 billion USD in Brazil (Wen et al., 2024), 308 million USD in Rwanda, and 1.38 billion USD in Ghana (Fisher et al., 2021). This monetization of health impacts helps to generate public awareness. Combating environmental pollution, minimizing economic costs, reducing regional disparities, and safeguarding citizens' right to health is a worldwide imperative.

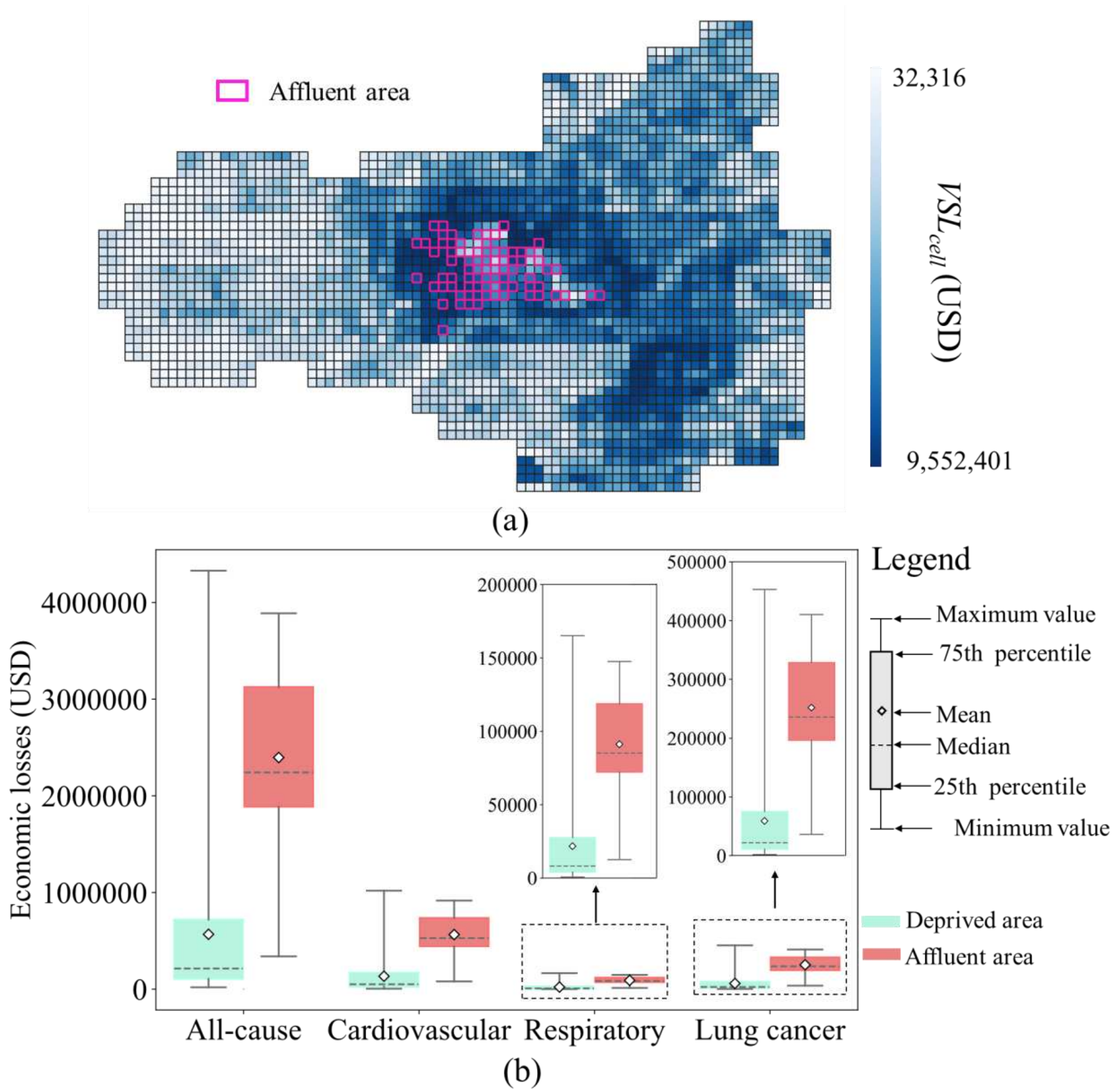

Figure 5 The economic costs of $PM_{2.5}$ health impacts. (a) The distribution of VSL_{cell}. (b) The economic costs for four health outcomes.

4. Discussion

4.1. Disparities in deprived and affluent areas

Areas with high housing prices were fully covered by monitoring and used as the baseline for our analysis. A certain percentage of the deprived population was exposed to pollution levels exceeding the highest concentrations in affluent areas in each season. The proportion of deaths attributable to four health outcomes was higher in low housing price areas. The deprived areas had a larger population but lower economic costs. This reveals an uneven distribution of pollution exposure, health impacts, and economic costs across the population. Deprived communities are exposed to higher levels of environmental pollution and health risks, which has also been confirmed in other studies (Tonne et al., 2018; Fairburn et al., 2019; Bramble et al., 2023).

Are there inequalities within deprived or affluent areas? We have calculated this according to **Equations (11) (12)**. The G_s is 2.28% for affluent areas and 9.12% for deprived areas, indicating disparities in pollution exposure are larger within deprived areas. Deprived communities face a more complex situation. Communities with lower socio-economic positions have higher health risks than their external counterparts, with larger internal variations as well. In deprived areas, some inhabitants dwell within the confines of mountains and forests, where the underdeveloped road network and low levels of modern infrastructure contribute to a lower degree of pollution exposure. Others reside in self-built houses adjacent to farmland, where agricultural machinery may be one of the primary sources of pollutant emissions. According to the Cangzhou Statistical Yearbook in 2021, the total power of diesel engines in Cang County (where high housing price area are concentrated) and Xinhua and Yunhe Districts (where low housing prices are concentrated) was 986,480 kW and 59,009 kW, respectively, as detailed in **Figure S6**. Moreover, due to the prohibition of trucks entering the central urban areas, the demand for transportation necessitates their operation on the peripheral suburban road networks of the city. According to a field study, the number of trucks passing through the roads surrounding low housing residential area in Cang County exceeds 150 per hour (more details can be seen in **Figure S7**), which increases the severe pollution to the socioeconomically disadvantaged groups.

Environmental protections tend to be more favorable towards communities with high socio-economic positions. For example, fixed monitoring stations and effective pollution warning systems are primarily concentrated in the central areas of small and medium-sized cities due to the high costs of installation and maintenance. As illustrated in **Figure 6**, the density of these stations is only 0.00343 per square kilometer in the study area, leaving large regions unmonitored. Compared to the high-resolution pollution heatmap generated through mobile monitoring (**Figure 3 (a)**), many pollution hotspots remain undetected by the fixed network. However, as more urban populations reside in small and medium-sized cities (Fahmi et al., 2014), expanding the spatial coverage of pollution monitoring and implementing refined health impact assessments are essential steps for addressing environmental pollution and reducing health risks. For instance, creating air pollution monitoring networks by combining mobile monitoring methods. Concentration and health risk heat maps can be developed to identify areas of high pollution levels and high health risk, such as **Figure 3 (a)** and **Figure 4 (a)**. Moreover, in the suburbs of small and medium-sized cities, agricultural activities dominate the outskirts (Pan and Wang, 2022). Strengthening emission management for agricultural equipment in deprived areas is necessary to prevent direct exposure to pollutants.

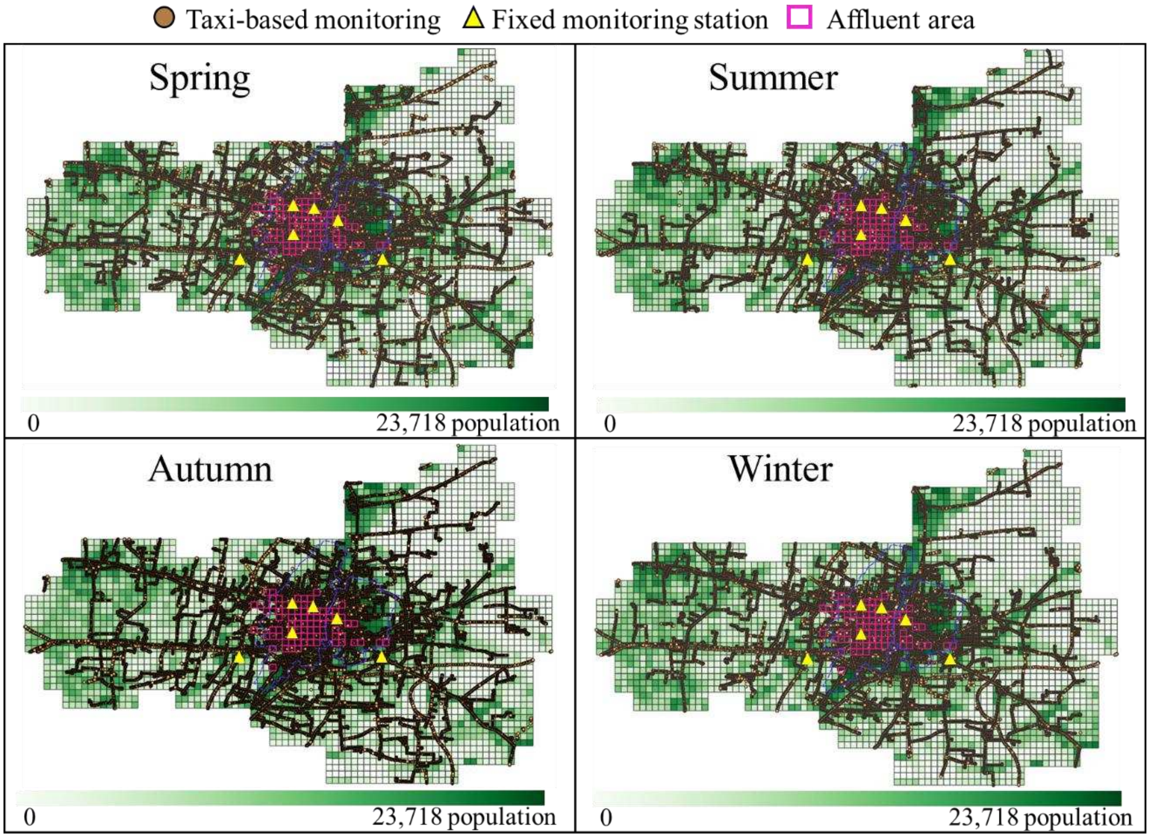

Figure 6 Distribution of mobile monitoring and fixed monitoring stations.

4.2. Health impacts analysis of demographics

Health impacts are unevenly distributed across demographic characteristics. The exposure response coefficient β values for four health outcomes were obtained from different cohort studies (Chen et al., 2018; Vodonos et al., 2018; Guo et al., 2020a, 2016; Wang et al., 2020; Yang et al., 2020). Since the World Health Organization (WHO) defines people aged 65 years and over as older people (Organization, 2015), the population was divided into three age groups: 0-64 years, 65-74 years, and >75 years.

The relative risks (RRs) for four health outcomes vary by age group. The RRs are lower for individuals under 65 years old, while those aged 65-74 have more burdens of $PM_{2.5}$ attributable all-cause, cardiovascular and lung cancer mortality. And the RRs are lower for individuals over 75 years old. The feasible reason is that susceptible residents die before reaching the 75 and older age group, and individuals over 65 are at greater risk of $PM_{2.5}$ exposure compared to younger populations (Chen et al., 2018). Additionally, based on the gender-specific RRs, males are at greater risk of $PM_{2.5}$-related mortality of all-cause, cardiovascular disease and lung cancer. Significant effects of $PM_{2.5}$ on mortality of respiratory causes were observed in females. And more details can be seen in **Figure S9**.

4.3. The land use and pollution exposure disparities

In our study, pollution exposure and health risks were lower in affluent areas (mainly located in city centers), while higher in deprived areas (mainly located in suburban areas), shown in **Figure 3 (a)** and **Figure 4 (a)**. The relationship between $PM_{2.5}$ concentration, land use, and road length were quantified by using Geographically Weighted Regression (GWR) model. Following the steps outlined in **Figure 7**, spatial autocorrelation tests, influencing factors selection, and model construction were conducted. The result shows that roadside $PM_{2.5}$ concentrations exhibit a positive correlation with industrial area, expressway length, and branch road length, while showing a negative correlation with residential areas (more details can be seen in **Supplementary Materials**).

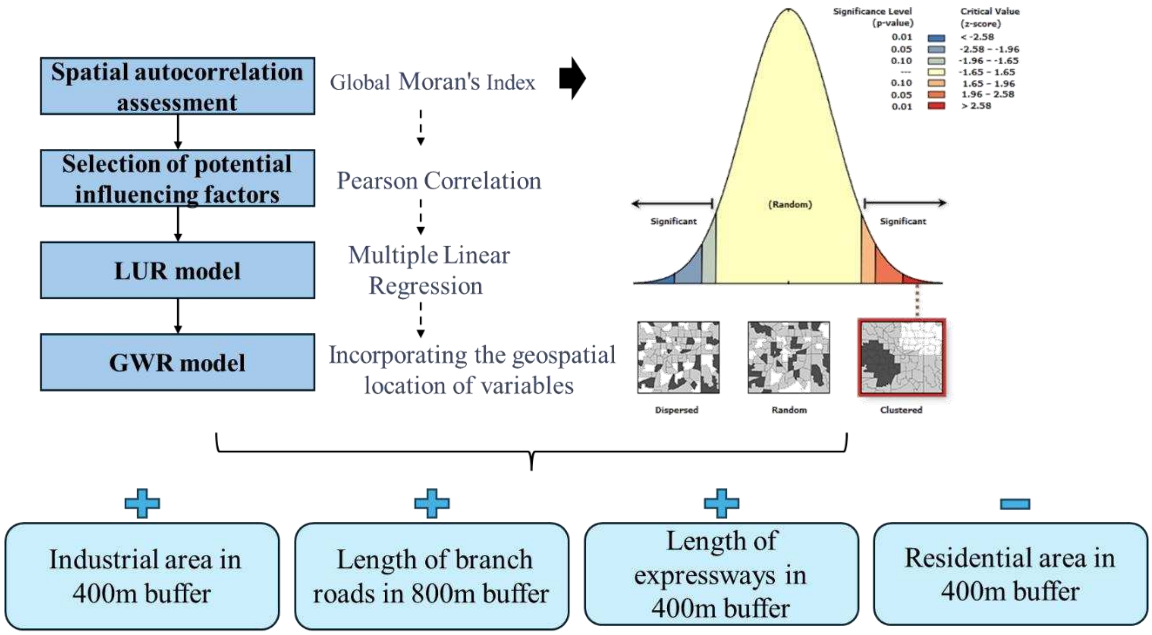

Figure 7 The steps and results for GWR model building.

Cangzhou is a typical medium-sized city in China, characterized by a developed urban core while industrial land is distributed in the surrounding areas far from the city center. Populations with lower socioeconomic status tend to prefer low-cost housing near industrial zones (Hanna, 2007; Sharghi et al., 2022). This pattern is observed in similar developing country cities like China (Ding et al., 2023), and south-central Chile (Romero et al., 2012), where suburbs exhibit higher health risks compared to central areas. Additionally, the import and export activities in industrial areas increase truck traffic, further contributing to higher $PM_{2.5}$ emissions. The road fleet configurations in the central areas include no trucks but their proportion is higher in the suburbs (over 20%), according to our field research.

We simulated a scenario where the industrial land area was reduced to 10% of its current size, resulting in a change in pollution concentration distribution. The $PM_{2.5}$ concentration decreased by an average of 2.2%. And the relative risks of all-cause, cardiovascular disease, respiratory disease, and lung cancer deaths decreased by 0.007, 0.008, 0.003, and 0.014, respectively (more details can be seen in **Supplementary Materials**).

Urban planning and facility distribution influence the distribution of population exposure to pollution and raises Environmental Justice concerns. Based on the GWR model, a negative correlation between pollution concentrations and residential areas was found, indicating that higher proportions of residential zones are associated with lower $PM_{2.5}$ concentrations. In areas with high housing prices, larger proportions of land, higher green coverage, and better isolation from surrounding regions effectively reduce particulate pollution and improve human health (Bi et al., 2022). Wealthier populations tend to choose to reside in areas with better air quality, far from degraded or polluted zones, having higher security against risks and natural hazards (Romero et al., 2012). In some developed cities, employment and commercial activities have shifted to suburban areas. Affluent individuals have moved to the suburbs, seeking lower population density, higher living standards, and greater comfort. In contrast, disadvantaged groups are often forced to live in the urban core (Daskalova and Slaev, 2015; Morris, 2019). Diverse exposure patterns exist within regions or countries. For example, air pollution levels are higher in central Shenzhen, China, compared to rural areas (Guo et al., 2020b). These disparities highlight the importance of investigating exposure differences across diverse contexts. A deeper understanding of local air pollution exposure inequalities is crucial for developing targeted policies to address health inequities. Environmental policymakers should shift their perspective to emphasize the uneven spatial distribution of building environment, air pollution, and health impacts in an effort to reduce regional disparities.

5. Conclusions

In this study, disparities in pollution exposure, health effects, and related economic costs between affluent and deprived areas were estimated by using the taxi-based mobile atmospheric monitoring system in a medium-sized city in China. The results showed that the mean value cannot capture the full extent of inequalities in pollution exposure. The roadside $PM_{2.5}$ concentrations in some deprived areas exceeded the maximum concentrations in affluent areas. The relative risks of health hazards due to $PM_{2.5}$ are higher in deprived communities. Health inequalities exist among communities with different socio-economic positions. Given that the economic costs are higher in affluent areas, people with high socio-economic positions are more willing to pay for protecting their health. Existing environmental policies are pollution-centered, focusing only on pollutants and their sources while neglecting the human or health-oriented approach. A shift should be made in perspective by emphasizing patterns of local disparities in air pollution exposure and endeavoring to reduce regional disparities (e.g., between deprived and affluent areas).

However, there are still limitations in our study. We only used housing price data to distinguish between deprived and affluent areas, as income data is challenging to obtain given privacy concerns. In addition, we measured economic costs in Cangzhou based on existing studies of other regions in China and did not conduct localized willingness-to-pay surveys. Future studies could enhance localized surveys and develop pollutant concentration prediction models to characterize pollution levels in areas not covered by stationary monitoring.

Acknowledgements

This work was supported by the Fundamental Research Funds for the Central Universities [grant number 2023YJS033]; the National Natural Science Foundation of China [grant number 52272340].

Cangzhou City Air Pollution Hotspot Grid Management Office; Environmental Defense Fund (EDF); Dust Control Laboratory of Shandong University; Institute of Atmospheric Environment, Chinese Research Academy of Environmental Sciences and Beijing Huanding Environmental Big Data Institute provide data support for this study.

References

Antonczak, B., Thompson, T.M., DePaola, M.W., Rowangould, G., 2023. 2020 Near-roadway population census, traffic exposure and equity in the United States. Transp Res D Transp Environ 125, 103965. https://doi.org/https://doi.org/10.1016/j.trd.2023.103965

Apte, J.S., Messier, K.P., Gani, S., Brauer, M., Kirchstetter, T.W., Lunden, M.M., Marshall, J.D., Portier, C.J., Vermeulen, R.C.H., Hamburg, S.P., 2017. High-Resolution Air Pollution Mapping with Google Street View Cars: Exploiting Big Data. Environ Sci Technol 51, 6999–7008. https://doi.org/10.1021/acs.est.7b00891

Atalay, K., Edwards, R., 2022. House prices, housing wealth and financial well-being. J Urban Econ 129, 103438. https://doi.org/https://doi.org/10.1016/j.jue.2022.103438

Atkinson, A.B., 1970. On the measurement of inequality. J Econ Theory 2, 244–263. https://doi.org/https://doi.org/10.1016/0022-0531(70)90039-6

Badland, H., Pearce, J., 2019. Liveable for whom? Prospects of urban liveability to address health inequities. Soc Sci Med 232, 94–105. https://doi.org/https://doi.org/10.1016/j.socscimed.2019.05.001

Belis, C.A., Matkovic, V., Ballocci, M., Jevtic, M., Millo, G., Mata, E., Van Dingenen, R., 2023. Assessment of health impacts and costs attributable to air pollution in urban areas using two different approaches. A case study in the Western Balkans. Environ Int 182, 108347. https://doi.org/https://doi.org/10.1016/j.envint.2023.108347

Berdegué, J.A., Soloaga, I., 2018. Small and medium cities and development of Mexican rural areas. World Dev 107, 277–288. https://doi.org/https://doi.org/10.1016/j.worlddev.2018.02.007

Berger, D., Guerrieri, V., Lorenzoni, G., Vavra, J., 2018. House prices and consumer spending. Rev Econ Stud 85, 1502–1542.

Bi, S., Dai, F., Chen, M., Xu, S., 2022. A new framework for analysis of the morphological spatial patterns of urban green space to reduce PM2. 5 pollution: A case study in Wuhan, China. Sustain Cities Soc 82, 103900.

Bramble, K., Blanco, M.N., Doubleday, A., Gassett, A.J., Hajat, A., Marshall, J.D., Sheppard, L., 2023. Exposure disparities by income, race and ethnicity, and historic redlining grade in the greater Seattle area for ultrafine particles and other air pollutants. Environ Health Perspect 131, 077004.

Burnett, R.T., Pope III, C.A., Ezzati, M., Olives, C., Lim, S.S., Mehta, S., Shin, H.H., Singh, G., Hubbell, B., Brauer, M., 2014. An integrated risk function for estimating the global burden of disease attributable to ambient fine particulate matter exposure. Environ Health Perspect 122, 397–403.

Chen, C., Zhu, P., Lan, L., Zhou, L., Liu, R., Sun, Q., Ban, J., Wang, W., Xu, D., Li, T., 2018. Short-term exposures to PM2. 5 and cause-specific mortality of cardiovascular health in China. Environ Res 161, 188–194.

Chen, R., Yin, P., Meng, X., Liu, C., Wang, L., Xu, X., Ross, J.A., Tse, L.A., Zhao, Z., Kan, H., 2017. Fine particulate air pollution and daily mortality. A nationwide analysis in 272 Chinese cities. Am J Respir Crit Care Med 196, 73–81.

Chowdhury, S., Dey, S., 2016. Cause-specific premature death from ambient PM2. 5 exposure in India: Estimate adjusted for baseline mortality. Environ Int 91, 283–290.

Coffee, N.T., Lockwood, T., Hugo, G., Paquet, C., Howard, N.J., Daniel, M., 2013. Relative residential property value as a socio-economic status indicator for health research. Int J Health Geogr 12, 1–10.

Daskalova, D., Slaev, A.D., 2015. Diversity in the suburbs: Socio-spatial segregation and mix in post-socialist Sofia. Habitat Int 50, 42–50. https://doi.org/https://doi.org/10.1016/j.habitatint.2015.07.007

deSouza, P., Wang, A., Machida, Y., Duhl, T., Mora, S., Kumar, P., Kahn, R., Ratti, C., Durant, J.L., Hudda, N., 2023. Evaluating the Performance of Low-Cost PM2. 5 Sensors in Mobile Settings. Environ Sci Technol 57, 15401–15411.

Ding, Y., Wang, C., Wang, J., Wang, P., Huang, L., 2023. Revealing the impact of built environment, air pollution and housing price on health inequality: an empirical analysis of Nanjing, China. Front Public Health 11, 1153021.

Fahmi, F.Z., Hudalah, D., Rahayu, P., Woltjer, J., 2014. Extended urbanization in small and medium-sized cities: The case of Cirebon, Indonesia. Habitat Int 42, 1–10.

Fairburn, J., Schüle, S.A., Dreger, S., Karla Hilz, L., Bolte, G., 2019. Social inequalities in exposure to ambient air pollution: a systematic review in the WHO European region. Int J Environ Res Public Health 16, 3127.

Fang, D., Wang, Q., Li, H., Yu, Y., Lu, Y., Qian, X., 2016. Mortality effects assessment of ambient PM2. 5 pollution in the 74 leading cities of China. Science of the Total Environment 569, 1545–1552.

Fang, X., Ma, Q., Wu, L., Liu, X., 2023. Distributional environmental justice of residential walking space: The lens of urban ecosystem services supply and demand. J Environ Manage 329, 117050. https://doi.org/https://doi.org/10.1016/j.jenvman.2022.117050

Fisher, S., Bellinger, D.C., Cropper, M.L., Kumar, P., Binagwaho, A., Koudenoukpo, J.B., Park, Y., Taghian, G., Landrigan, P.J., 2021. Air pollution and development in Africa: impacts on health, the economy, and human capital. Lancet Planet Health 5, e681–e688. https://doi.org/https://doi.org/10.1016/S2542-5196(21)00201-1

Giannadaki, D., Giannakis, E., Pozzer, A., Lelieveld, J., 2018. Estimating health and economic benefits of reductions in air pollution from agriculture. Science of The Total Environment 622–623, 1304–1316. https://doi.org/https://doi.org/10.1016/j.scitotenv.2017.12.064

Guo, H., Li, W., Wu, J., 2020a. Ambient PM2. 5 and annual lung cancer incidence: a nationwide study in 295 Chinese counties. Int J Environ Res Public Health 17, 1481.

Guo, H., Li, W., Yao, F., Wu, J., Zhou, X., Yue, Y., Yeh, A.G.O., 2020b. Who are more exposed to PM2.5 pollution: A mobile phone data approach. Environ Int 143, 105821. https://doi.org/https://doi.org/10.1016/j.envint.2020.105821

Guo, X.R., Cheng, S.Y., Chen, D.S., Zhou, Y., Wang, H.Y., 2010. Estimation of economic costs of particulate air pollution from road transport in China. Atmos Environ 44, 3369–3377. https://doi.org/https://doi.org/10.1016/j.atmosenv.2010.06.018

Guo, Y., Zeng, H., Zheng, R., Li, S., Barnett, A.G., Zhang, S., Zou, X., Huxley, R., Chen, W., Williams, G., 2016. The association between lung cancer incidence and ambient air pollution in China: A spatiotemporal analysis. Environ Res 144, 60–65.

Hanna, B.G., 2007. House values, incomes, and industrial pollution. J Environ Econ Manage 54, 100–112.

Hao, X., Hu, X., Liu, T., Wang, C., Wang, L., 2022. Estimating urban PM2.5 concentration: An analysis on the nonlinear effects of explanatory variables based on gradient boosted regression tree. Urban Clim 44, 101172. https://doi.org/https://doi.org/10.1016/j.uclim.2022.101172

Hoek, G., Beelen, R., De Hoogh, K., Vienneau, D., Gulliver, J., Fischer, P., Briggs, D., 2008. A review of land-use regression models to assess spatial variation of outdoor air pollution. Atmos Environ 42, 7561–7578.

Hsu, A., Sheriff, G., Chakraborty, T., Manya, D., 2021. Disproportionate exposure to urban heat island intensity across major US cities. Nat Commun 12, 2721.

Islam, Md.R., McGillivray, M., 2020. Wealth inequality, governance and economic growth. Econ Model 88, 1–13. https://doi.org/https://doi.org/10.1016/j.econmod.2019.06.017

Kim, S., Ko, Y., Jang, K., 2024. Air pollution, perceived health risk, and trip decision-making: Environmental justice considerations. Cities 149, 104949. https://doi.org/https://doi.org/10.1016/j.cities.2024.104949

Kingham, S., Pearce, J., Zawar-Reza, P., 2007. Driven to injustice? Environmental justice and vehicle pollution in Christchurch, New Zealand. Transp Res D Transp Environ 12, 254–263. https://doi.org/https://doi.org/10.1016/j.trd.2007.02.004

Li, V.O.K., Han, Y., Lam, J.C.K., Zhu, Y., Bacon-Shone, J., 2018. Air pollution and environmental injustice: Are the socially deprived exposed to more PM2. 5 pollution in Hong Kong? Environ Sci Policy 80, 53–61.

Lim, S.S., Vos, T., Flaxman, A.D., Danaei, G., Shibuya, K., Adair-Rohani, H., AlMazroa, M.A., Amann, M., Anderson, H.R., Andrews, K.G., Aryee, M., Atkinson, C., Bacchus, L.J., Bahalim, A.N., Balakrishnan, K., Balmes, J., Barker-Collo, S., Baxter, A., Bell, M.L., Blore, J.D., Blyth, F., Bonner, C., Borges, G., Bourne, R., Boussinesq, M., Brauer, M., Brooks, P., Bruce, N.G., Brunekreef, B., Bryan-Hancock, C., Bucello, C., Buchbinder, R., Bull, F., Burnett, R.T., Byers, T.E., Calabria, B., Carapetis, J., Carnahan, E., Chafe, Z., Charlson, F., Chen, H., Chen, J.S., Cheng, A.T.-A., Child, J.C., Cohen, A., Colson, K.E., Cowie, B.C., Darby, S., Darling, S., Davis, A., Degenhardt, L., Dentener, F., Des Jarlais, D.C., Devries, K., Dherani, M., Ding, E.L., Dorsey, E.R., Driscoll, T., Edmond, K., Ali, S.E., Engell, R.E., Erwin, P.J., Fahimi, S., Falder, G., Farzadfar, F., Ferrari, A., Finucane, M.M., Flaxman, S., Fowkes, F.G.R., Freedman, G., Freeman, M.K., Gakidou, E., Ghosh, S., Giovannucci, E., Gmel, G., Graham, K., Grainger, R., Grant, B., Gunnell, D., Gutierrez, H.R., Hall, W., Hoek, H.W., Hogan, A., Hosgood, H.D., Hoy, D., Hu, H., Hubbell, B.J., Hutchings, S.J., Ibeanusi, S.E., Jacklyn, G.L., Jasrasaria, R., Jonas, J.B., Kan, H., Kanis, J.A., Kassebaum, N., Kawakami, N., Khang, Y.-H., Khatibzadeh, S., Khoo, J.-P., Kok, C., Laden, F., Lalloo, R., Lan, Q., Lathlean, T., Leasher, J.L., Leigh, J., Li, Y., Lin, J.K., Lipshultz, S.E., London, S., Lozano, R., Lu, Y., Mak, J., Malekzadeh, R., Mallinger, L., Marcenes, W., March, L., Marks, R., Martin, R., McGale, P., McGrath, J., Mehta, S., Memish, Z.A., Mensah, G.A., Merriman, T.R., Micha, R., Michaud, C., Mishra, V., Hanafiah, K.M., Mokdad, A.A., Morawska, L., Mozaffarian, D., Murphy, T., Naghavi, M., Neal, B., Nelson, P.K., Nolla, J.M., Norman, R., Olives, C., Omer, S.B., Orchard, J., Osborne, R., Ostro, B., Page, A., Pandey, K.D., Parry, C.D.H., Passmore, E., Patra, J., Pearce, N., Pelizzari, P.M., Petzold, M., Phillips, M.R., Pope, D., Pope, C.A., Powles, J., Rao, M., Razavi, H., Rehfuess, E.A., Rehm, J.T., Ritz, B., Rivara, F.P., Roberts, T., Robinson, C., Rodriguez-Portales, J.A., Romieu, I., Room, R., Rosenfeld, L.C., Roy, A., Rushton, L., Salomon, J.A., Sampson, U., Sanchez-Riera, L., Sanman, E., Sapkota, A., Seedat, S., Shi, P., Shield, K., Shivakoti, R., Singh, G.M., Sleet, D.A., Smith, E., Smith, K.R., Stapelberg, N.J.C., Steenland, K., Stöckl, H., Stovner, L.J., Straif, K., Straney, L., Thurston, G.D., Tran, J.H., Van Dingenen, R., van Donkelaar, A., Veerman, J.L., Vijayakumar, L., Weintraub, R., Weissman, M.M., White, R.A., Whiteford, H., Wiersma, S.T., Wilkinson, J.D., Williams, H.C., Williams, W., Wilson, N., Woolf, A.D., Yip, P., Zielinski, J.M., Lopez, A.D., Murray, C.J.L., Ezzati, M., 2012. A comparative risk assessment of burden of disease and injury attributable to 67 risk factors and risk factor clusters in 21 regions, 1990–2010: a systematic analysis for the Global Burden of Disease Study 2010. The Lancet 380, 2224–2260. https://doi.org/https://doi.org/10.1016/S0140-6736(12)61766-8

Lin, H., Ratnapradipa, K., Wang, X., Zhang, Y., Xu, Y., Yao, Z., Dong, G., Liu, T., Clark, J., Dick, R., Xiao, J., Zeng, W., Li, X., Qian, Z. (Min), Ma, W., 2017. Hourly peak concentration measuring the PM2.5-mortality association: Results from six cities in the Pearl River Delta study. Atmos Environ 161, 27–33. https://doi.org/https://doi.org/10.1016/j.atmosenv.2017.04.015

Määttänen, N., Terviö, M., 2014. Income distribution and housing prices: An assignment model approach. J Econ Theory 151, 381–410.

Maji, K.J., Ye, W.-F., Arora, M., Shiva Nagendra, S.M., 2018. PM2.5-related health and economic loss assessment for 338 Chinese cities. Environ Int 121, 392–403. https://doi.org/https://doi.org/10.1016/j.envint.2018.09.024

Manisalidis, I., Stavropoulou, E., Stavropoulos, A., Bezirtzoglou, E., 2020. Environmental and health impacts of air pollution: a review. Front Public Health 8, 14.

Marmot, M., 2020. Health equity in England: the Marmot review 10 years on. Bmj 368.

Martin, R. V, Brauer, M., van Donkelaar, A., Shaddick, G., Narain, U., Dey, S., 2019. No one knows which city has the highest concentration of fine particulate matter. Atmos Environ X 3, 100040.

Mirkatouli, J., Samadi, R., Hosseini, A., 2018. Evaluating and analysis of socio-economic variables on land and housing prices in Mashhad, Iran. Sustain Cities Soc 41, 695–705.

Molitor, J., Su, J.G., Molitor, N.-T., Rubio, V.G., Richardson, S., Hastie, D., Morello-Frosch, R., Jerrett, M., 2011. Identifying vulnerable populations through an examination of the association between multipollutant profiles and poverty. Environ Sci Technol 45, 7754–7760.

Morris, E.A., 2019. Do cities or suburbs offer higher quality of life? Intrametropolitan location, activity patterns, access, and subjective well-being. Cities 89, 228–242. https://doi.org/https://doi.org/10.1016/j.cities.2019.02.012

Munir, M.M., Adrian, M., Saputra, C., Lestari, P., 2022. Utilizing low-cost mobile monitoring to estimate the PM2. 5 inhaled dose in urban environment. Aerosol Air Qual Res 22, 220079.

OECD, 2014. The Cost of Air Pollution. OECD. https://doi.org/10.1787/9789264210448-en

Orellano, P., Reynoso, J., Quaranta, N., Bardach, A., Ciapponi, A., 2020. Short-term exposure to particulate matter (PM10 and PM2. 5), nitrogen dioxide (NO2), and ozone (O3) and all-cause and cause-specific mortality: Systematic review and meta-analysis. Environ Int 142, 105876.

Organization, W.H., 2015. World report on ageing and health. World Health Organization.

Pan, J., Wang, H., 2022. Analysis on the Development of Rural Small and Medium Enterprises and New Urbanization. China's Reform and New Urbanization 99–115.

Pascal, M., Corso, M., Chanel, O., Declercq, C., Badaloni, C., Cesaroni, G., Henschel, S., Meister, K., Haluza, D., Martin-Olmedo, P., 2013. Assessing the public health impacts of urban air pollution in 25 European cities: results of the Aphekom project. Science of the Total Environment 449, 390–400.

Pisoni, E., Dominguez-Torreiro, M., Thunis, P., 2022. Inequality in exposure to air pollutants: A new perspective. Environ Res 212, 113358. https://doi.org/https://doi.org/10.1016/j.envres.2022.113358

Pisoni, E., Thunis, P., De Meij, A., Wilson, J., Bessagnet, B., Crippa, M., Guizzardi, D., Belis, C.A., Van Dingenen, R., 2023. Modelling the air quality benefits of EU climate mitigation policies using two different PM2.5-related health impact methodologies. Environ Int 172, 107760. https://doi.org/https://doi.org/10.1016/j.envint.2023.107760

Qiu, Z., Xu, X., Song, J., Luo, Y., Zhao, R., Zhou, B.X.W., Li, X., Hao, Y., 2017. Pedestrian exposure to traffic PM on different types of urban roads: A case study of Xi'an, China. Sustain Cities Soc 32, 475–485. https://doi.org/https://doi.org/10.1016/j.scs.2017.04.007

Romero, H., Vásquez, A., Fuentes, C., Salgado, M., Schmidt, A., Banzhaf, E., 2012. Assessing urban environmental segregation (UES). The case of Santiago de Chile. Ecol Indic 23, 76–87.

Rowangould, G.M., 2013. A census of the US near-roadway population: Public health and environmental justice considerations. Transp Res D Transp Environ 25, 59–67. https://doi.org/https://doi.org/10.1016/j.trd.2013.08.003

Sharghi, A., Nourtaghani, A., Ramzanpour, M., Gorji, R.B., 2022. Low-income housing location based on affordable criteria Using AHP Model and GIS Technique (Case Study: Babolsar City). Environ Dev Sustain 24, 10337–10377.

Stampfer, O., Austin, E., Ganuelas, T., Fiander, T., Seto, E., Karr, C.J., 2020. Use of low-cost PM monitors and a multi-wavelength aethalometer to characterize PM2. 5 in the Yakama Nation reservation. Atmos Environ 224, 117292.

Sun, C., Kahn, M.E., Zheng, S., 2017. Self-protection investment exacerbates air pollution exposure inequality in urban China. Ecological economics 131, 468–474.

Sun, X., Zhang, R., Wang, G., 2022. Spatial-temporal evolution of health impact and economic loss upon exposure to PM2. 5 in China. Int J Environ Res Public Health 19, 1922.

Tao, Y., Chai, Y., Zhang, X., Yang, J., Kwan, M.-P., 2021. Mobility-based environmental justice: Understanding housing disparity in real-time exposure to air pollution and momentary psychological stress in Beijing, China. Soc Sci Med 287, 114372. https://doi.org/https://doi.org/10.1016/j.socscimed.2021.114372

Targino, A.C., Gibson, M.D., Krecl, P., Rodrigues, M.V.C., dos Santos, M.M., de Paula Corrêa, M., 2016. Hotspots of black carbon and PM2.5 in an urban area and relationships to traffic characteristics. Environmental Pollution 218, 475–486. https://doi.org/https://doi.org/10.1016/j.envpol.2016.07.027

Tonne, C., Milà, C., Fecht, D., Alvarez, M., Gulliver, J., Smith, J., Beevers, S., Anderson, H.R., Kelly, F., 2018. Socioeconomic and ethnic inequalities in exposure to air and noise pollution in London. Environ Int 115, 170–179.

United Nations, 2019. The sustainable development goals report 2019, The Sustainable Development Goals Report 2016.

US, E., 2019. Integrated science assessment (ISA) for particulate matter (final report, Dec 2019). US Environ. Prot. Agency.

Vodonos, A., Awad, Y.A., Schwartz, J., 2018. The concentration-response between long-term PM2. 5 exposure and mortality; A meta-regression approach. Environ Res 166, 677–689.

Wang, B., Eum, K.-D., Kazemiparkouhi, F., Li, C., Manjourides, J., Pavlu, V., Suh, H., 2020. The impact of long-term PM 2.5 exposure on specific causes of death: Exposure-response curves and effect modification among 53 million US Medicare beneficiaries. Environmental Health 19, 1–12.

Wang, J., Zhang, L., Niu, X., Liu, Z., 2020. Effects of PM2.5 on health and economic loss: Evidence from Beijing-Tianjin-Hebei region of China. J Clean Prod 257, 120605. https://doi.org/https://doi.org/10.1016/j.jclepro.2020.120605

Wang, L., Wu, Y., Wang, Y., Yu, L., Song, G., 2024. Modeling Urban-Rural health disparities using a Taxi-Based mobile atmospheric monitoring system. Transp Res D Transp Environ 129, 104152.

Wen, B., Ademi, Z., Wu, Y., Xu, R., Yu, P., Ye, T., Coêlho, M. de S.Z.S., Saldiva, P.H.N., Guo, Y., Li, S., 2024. Ambient PM2.5 and productivity-adjusted life years lost in Brazil: a national population-based study. J Hazard Mater 467, 133676. https://doi.org/https://doi.org/10.1016/j.jhazmat.2024.133676

WHO, 2021. WHO global air quality guidelines: particulate matter (PM2. 5 and PM10), ozone, nitrogen dioxide, sulfur dioxide and carbon monoxide. World Health Organization.

WHO, 2016. Ambient air pollution: A global assessment of exposure and burden of disease.

WHO, 2006. WHO air quality guidelines for particulate matter, ozone, nitrogen dioxide and sulfur dioxide: Global assessment 2005: summary of risk assessment.

Wu, Y., Wang, L., Wang, Y., Song, G., Yu, L., 2023. Health effects of exposure to particulate matter and physical activity by individual sustainable commuting modes. J Clean Prod 397, 136524.

Wu, Y., Wang, Y., Wang, L., Song, G., Gao, J., Yu, L., 2020. Application of a taxi-based mobile atmospheric monitoring system in Cangzhou, China. Transp Res D Transp Environ 86, 102449.

Yang, S., Fang, D., Chen, B., 2019. Human health impact and economic effect for PM2. 5 exposure in typical cities. Appl Energy 249, 316–325.

Yang, Y., Qi, J., Ruan, Z., Yin, P., Zhang, S., Liu, J., Liu, Y., Li, R., Wang, L., Lin, H., 2020. Changes in life expectancy of respiratory diseases from attaining daily PM2. 5 standard in China: a nationwide observational study. The Innovation 1.

Yin, H., Pizzol, M., Xu, L., 2017. External costs of PM2.5 pollution in Beijing, China: Uncertainty analysis of multiple health impacts and costs. Environmental Pollution 226, 356–369. https://doi.org/https://doi.org/10.1016/j.envpol.2017.02.029

Yu, Y.T., Xiang, S., Zhang, T., You, Y., Si, S., Zhang, S., Wu, Y., 2022. Evaluation of City-Scale Disparities in PM2. 5 Exposure Using Hyper-Localized Taxi-Based Mobile Monitoring. Environ Sci Technol 56, 13584–13594.

Zeng, X., Ruan, J., Li, K., Yu, C., Wang, Q., Ruan, F., 2024. Health impact and economic loss assessment of indoor PM2.5 pollution: A case during the COVID-19 lockdown period. Atmos Pollut Res 15, 101963. https://doi.org/https://doi.org/10.1016/j.apr.2023.101963

Zhang, B., Wu, B., Liu, J., 2020. PM2.5 pollution-related health effects and willingness to pay for improved air quality: Evidence from China’s prefecture-level cities. J Clean Prod 273, 122876. https://doi.org/https://doi.org/10.1016/j.jclepro.2020.122876

Zhang, M., Song, Y., Cai, X., Zhou, J., 2008. Economic assessment of the health effects related to particulate matter pollution in 111 Chinese cities by using economic burden of disease analysis. J Environ Manage 88, 947–954. https://doi.org/https://doi.org/10.1016/j.jenvman.2007.04.019